JOURNAL OF MATERIALS SCIENCE 28 (1993) 3247–3257

The recoil compressive strength of pitch-based carbon fibres

G. J. HAYES, D. D. EDIE, J. M. KENNEDY
Center for Advanced Engineering Fibers and their Composites, Earle Hall, Clemson University, Clemson, SC 29634, USA

The recoil compressive strengths of pitch-based carbon fibres with folded-radial and flat-layer textures were compared. Using the recoil test method, it was shown that the compressive strengths of pitch-based carbon fibres with folded-radial textures are superior to pitch-based carbon fibres with flat-layer textures at all modulus levels. Analysis of the failed fibre ends revealed that the folded-radial texture appeared to inhibit shearing of the basal planes. This may account for the superior compressive strengths of pitch-based carbon fibres with folded-radial textures. Procedural differences in the recoil test were shown to influence the calculated recoil compressive strength of pitch-based carbon fibres. Microscopic analysis of the recoil test specimens revealed that some energy is absorbed in the area where the fibre is secured to the support tab.

1. Introduction

The tensile strength and modulus of carbon fibres make them an attractive structural material in the aerospace, automotive and sporting goods industries. However, the use of carbon fibres as a structural component in high-performance applications is often limited by their compressive properties [1]. Among carbon fibres, pitch-based fibres exhibit the lowest compressive strengths, especially when compared to poly(acrylonitrile)-based (PAN-based) carbon fibres [1]. The factors that influence the mechanical properties of pitch-based carbon fibres must be identified before improvements in their compressive strengths can be made. Of particular interest is the influence of the fibre's texture and microstructure on its mechanical properties.

For the purposes of this paper, texture or morphology refers to the physical appearance of the fibres' structure observed in scanning electron microscope (SEM) photographs, and the fibre microstructure refers to its crystallographic structure. Many researchers have investigated the relationship between microstructure and texture of the fibre and fibre properties. For example, Endo [2] studied the differences between high Young's modulus ($E > 590$ GPa) pitch-based Carbonic (Kashima Oil Company) and Thornel (Amoco Performance Products, Inc.) fibres with SEM, transmission electron microscopy (TEM), and X-ray diffraction (XRD) techniques. He noted that the textural differences between the two types were similar to their microstructural differences. Fig. 1 shows Endo's proposed structure for the Thornel and Carbonic fibres. In these studies, Endo demonstrated that the Carbonic fibre, with a folded-layer microstructure and texture, had good preferred orientation in the direction of the fibre axis but still maintained a turbostratic crystalline structure even after high thermal treatment temperatures. However, the Thornel fibre, with a flat-layer microstructure and texture, was shown to have a higher degree of preferred orientation along the fibre axis than the Carbonic fibre and a crystalline structure more similar to that of graphite.

Endo [2] described the relationship between these microstructural and textural differences and the mechanical properties and failure mechanisms of each fibre type. The Thornel fibre has a higher modulus of elasticity than the Carbonic fibre due to its higher degree of orientation, whereas the Carbonic fibre has a superior tensile strength and failure strain in tension due to the influence of its microstructure on the failure mechanism. It is reasonable to assume that differences in microstructure may also lead to differences in the compressive properties of carbon fibres.

Dobb *et al.* [3] have related the recoil compressive properties and failure mechanisms of PAN- and pitch-based carbon fibres to differences in their microstructure. These authors reported that PAN-based fibres and low-modulus pitch-based fibres (Amoco P25) have higher recoil compressive strengths than high-modulus pitch-based fibres. The low recoil compressive strength of the high-modulus pitch-based fibres was associated with its sheet-like structure. This sheet-like structure, in contrast to the random structure of PAN-based fibres, was reported to facilitate shearing across basal planes, thereby reducing the fibre compressive strength.

In the present research, the apparent compressive strength of pitch-based carbon fibres with different textures was studied using the recoil method described by Allen [4]. Specifically, Thornel pitch-based carbon fibres with a flat-layer texture and Fiber G (E. I. du Pont de Nemours & Co. Inc.) pitch-based carbon

0022–2461

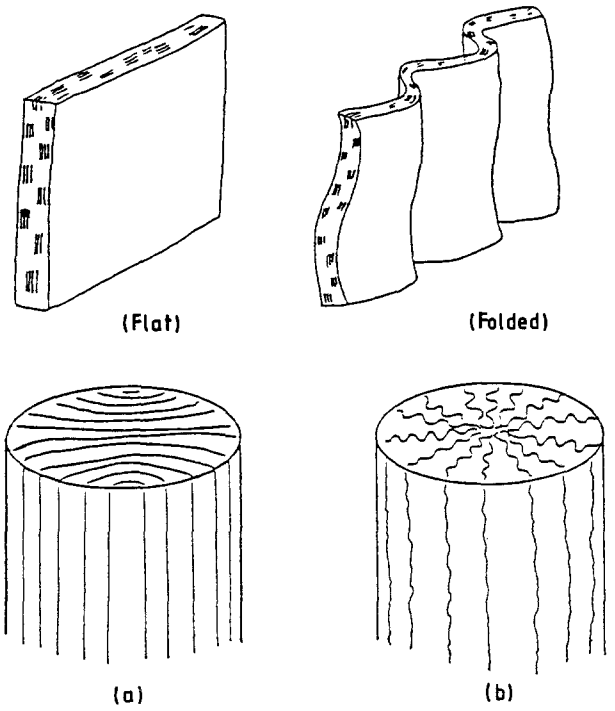

Figure 1 Endo's proposed structure for (a) Thornel and (b) Carbonic fibres [1].

fibres with a folded-radial texture were compared. Fig. 2 shows photographs of the texture of these fibres at high magnification. The figure shows that the texture of the Fiber G pitch-based carbon fibre is similar to the texture of the Kashima Oil Company Carbonic fibre. Endo [5] has reported that these fibres also have similar microstructures.

A hypothesis of the current research is that the structural differences between the Thornel and Fiber G carbon fibres will influence their mechanical properties, as Endo [2] observed with Thornel and Carbonic carbon fibres. In particular, the objective was to determine the effects of the observed textural differences on the compressive properties of these fibres.

2. Experimental procedure

2.1. Materials and equipment

To investigate the relationship between fibre texture and the fibre recoil compressive properties, carbon fibre samples were obtained from two fibre manufacturers, Amoco Performance Products, Inc. and E. I. du Pont de Nemours & Co. Inc. Both manufacturers supplied carbon fibres which were produced from petroleum-based mesophase pitch precursors. The

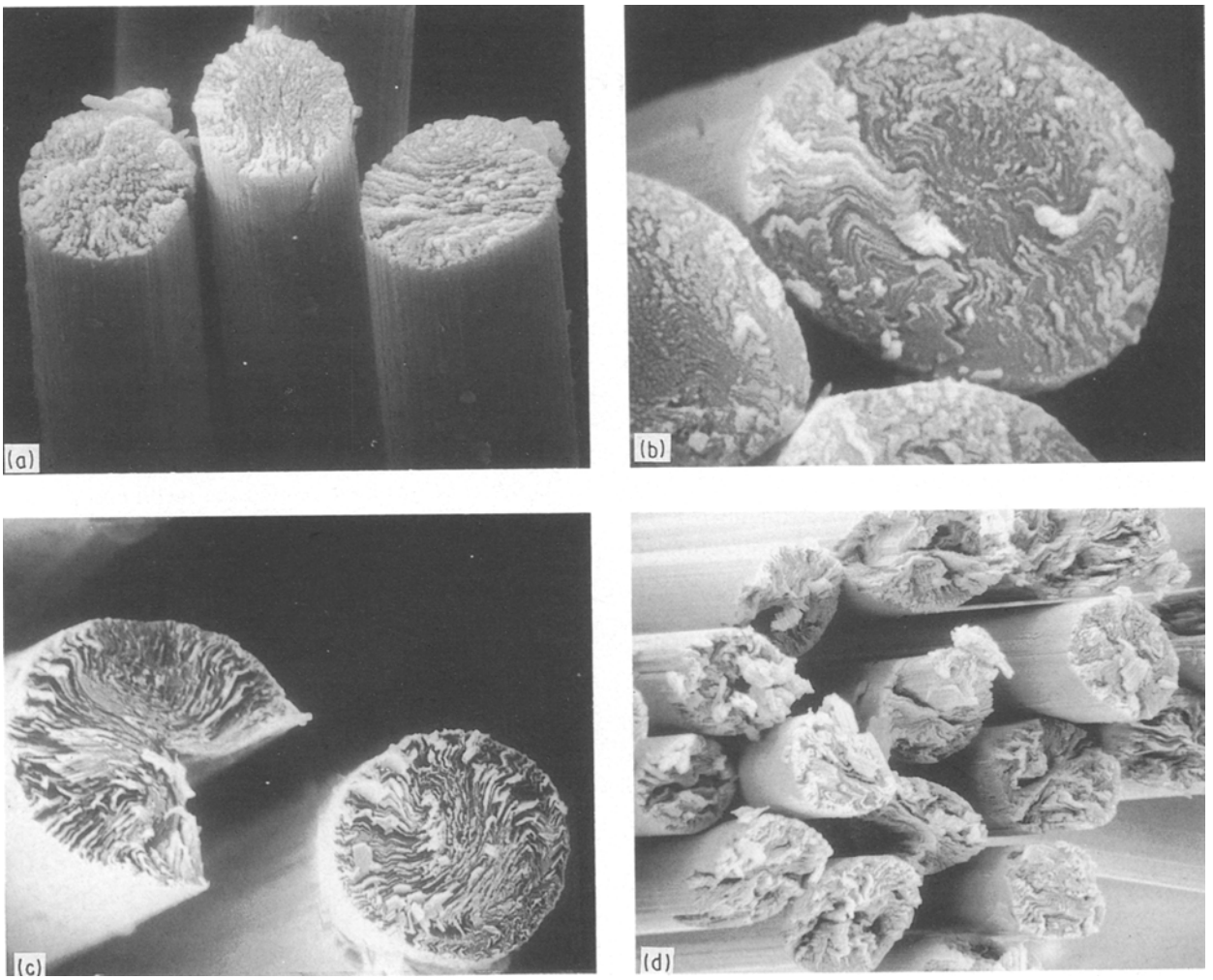

Figure 2 (a, c) Flat-layer texture of Thornel, and (b, d) folded-radial texture of Fiber G, pitch-based carbon fibres (a) P55, (b) E55, (c) P130, (d) E130.

fibres tested included the Amoco Thornel fibres, designated P25, P55, P75, P100, P120, and P130 (P130 is an experimental fibre which is not available commercially), and the du Pont Fiber G products, designated E35, E55, E75, E105, E120 and E130.

All fibres were tested as-received. Recoil and tensile tests were conducted in a Phoenix tensile testing system. Paper test tabs with 40 mm gauge lengths were used for recoil testing and tabs with 10, 20 and 40 mm gauge lengths were used for tensile testing. Microscopic studies of the failed fibres were conducted with an ETEC SEM at a 20 kV accelerating voltage.

2.2. Tensile testing procedure

Each type of fibre was subjected to single-filament tensile testing according to ASTM [6] testing procedures, with two exceptions. First, the machine compliance correction factor for each fibre designation was calculated by the method described by Li and Langley [7] using tensile data obtained from testing fibres at 10, 20 and 40 mm gauge lengths; between 20 and 25 fibres were tested at each gauge length. Second, the results are presented as the average of approximately 20 single filament tests conducted at 40 mm gauge length to minimize the influence of the machine compliance correction factor on the value of Young's modulus.

2.3. Recoil testing procedure

In the recoil test method, as with standard fibre tensile test methods, fibres were mounted on a paper support tab and secured with glue. The support tab was gripped by pneumatic jaws (grips) attached to a universal testing machine. Then, the side supports of the paper tab were severed by cutting with an electric hot-wire. The recoil test began by loading the fibre to a predetermined stress level. At this stress level, there was a corresponding amount of potential energy stored in the fibre in the form of strain energy. Next, the fibre recoil was initiated by cutting the fibre at the midpoint of the gauge length. Two methods to initiate the recoil were investigated in the present study; these two methods are shown in Fig. 3.

In the mechanical initiation technique described by Allen [4], a pair of surgical scissors were used to cut the fibre. In this method, the scissors must be carefully aligned with the midpoint of the gauge length and then operated with a steady, precise movement of the handles. If the fibre is not cut with the thin tips of the scissors, a lateral displacement will result which may influence the test results.

In the electrical initiation method described by Wang *et al.* [8], two electrodes were aligned on opposite sides of the fibre being tested at the midpoint of the gauge length. Typically, the distance between the electrodes was set at between 0.25 and 0.5 cm. Once the fibre and electrodes were aligned properly, the test was performed as described earlier. When the pre-selected stress level was attained, the electrical initiation was performed by imposing a 10 000 V potential across the electrodes. This large potential created an ionized path between the electrodes in the vicinity of the carbon fibre that produced an electric current. The carbon fibre was rapidly oxidized and/or ionized in the presence of this electric current until the recoil initiation occurred. Because adjustments can be made to the fibre and electrode positions to attain the desired alignment, a benefit of this method is that very small variations will occur when different operators conduct the test.

According to Allen [4], at the point where the fibre is cut, the stress goes to zero and the strain energy is converted to kinetic energy. Consequently, a stress wave front moves along the fibre towards the clamp and additional strain energy is converted to kinetic energy. When the clamp is reached, all of the strain energy has been converted to kinetic energy. Because the clamp is assumed to be rigid in Allen's [4] analysis, the kinetic energy reverts to strain energy and a compressive stress front is propagated back down the

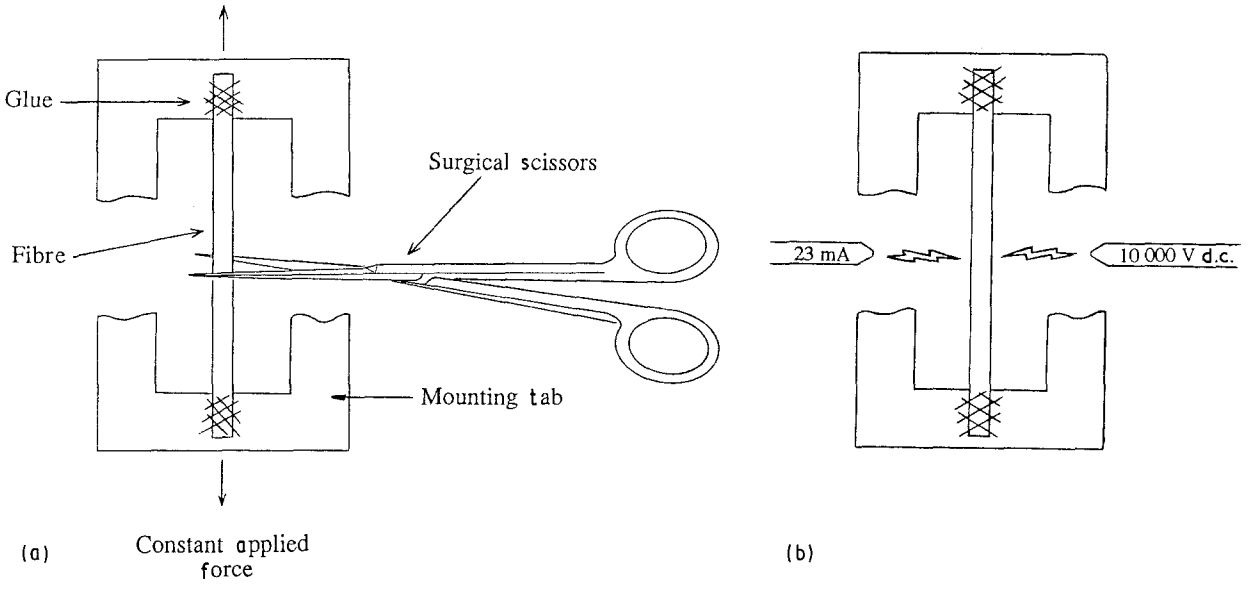

Figure 3 Recoil test initiation techniques. (a) Mechanical initiation, (b) electrical initiation.

fibre length. In the recoil test, the magnitude of the compressive stress is assumed to be equal to the applied stress. During the recoil, each half of the cut fibre will experience similar relaxation and compressive stresses because the entire fibre was assumed to be under a constant stress with a uniform strain-energy density. Therefore, each mounted fibre will produce two test results. For each variety of fibre studied, 45–100 single filaments were tested by the recoil method. Recoil stresses were calculated based on an average area for each fibre variety.

2.4. Data analysis

In the recoil test, the entire fibre is assumed to be under a constant stress. Furthermore, it is assumed that both halves of the cut fibre experience similar relaxation and compressive stresses and that there is no energy dissipated into the grip or into heat or sound. If the applied stress exceeds the critical recoil compressive strength of the fibre, compressive failure occurs. With brittle materials such as carbon fibres, failure is catastrophic and easily identified. In evaluating the results of a recoil test, both halves of the cut fibre are inspected for catastrophic failure. As Fig. 4 shows, a fibre either fails or survives the applied recoil compressive load.

When a fibre failure occurs by the recoil method, it is not possible to determine the actual compressive strength of that fibre because the applied stress could have exceeded the critical failure strength by an unknown amount. Therefore, it is not possible to obtain an average compressive strength directly from recoil test data. Several methods have been proposed in the literature to evaluate recoil test data [3, 4, 8–10]. However, these methods are not based on rigorous statistical considerations and, at best, only give approximate values for the recoil compressive strength.

Two methods to analyse the recoil test data were evaluated. In the first method described by Park [9], the data are grouped by stress ranges. Then, the percentage of fibre halves that survive the test is calculated for each range based on the total number of halves in the range. Next, a plot is constructed of the per cent survival as a function of the applied stress. The range is represented as the numerical average of the highest and lowest stress value in the range. The sample recoil compressive strength is estimated by calculating the stress corresponding to 50% survival. Selection of the stress ranges is somewhat subjective, but the driving force for a particular selection is based on the assumption that there is a smooth transition from 100% survival to 0% survival. This method is a good graphical technique for presenting recoil compressive stress data which cover a wide stress range.

In the second method used by Allen [4], Wang *et al.* [8] and Crasto and Kumar [10], the data are arranged in ascending order of load as in Table I. A range of stresses is identified over which the observations change from 100% survival to 100% failure (0% survival). Then, the recoil compressive strength is calculated as the average of the two endpoints of this range. Therefore, for the P130 fibre data shown in Table I, the recoil compressive strength is 410 MPa. This is the average of the stress at which the first failure occurs, 372 MPa, and the stress at which the last survival was recorded, 448 MPa. Individual points which appear to be outliers, such as the failure observed at 330 MPa, can be excluded from the range

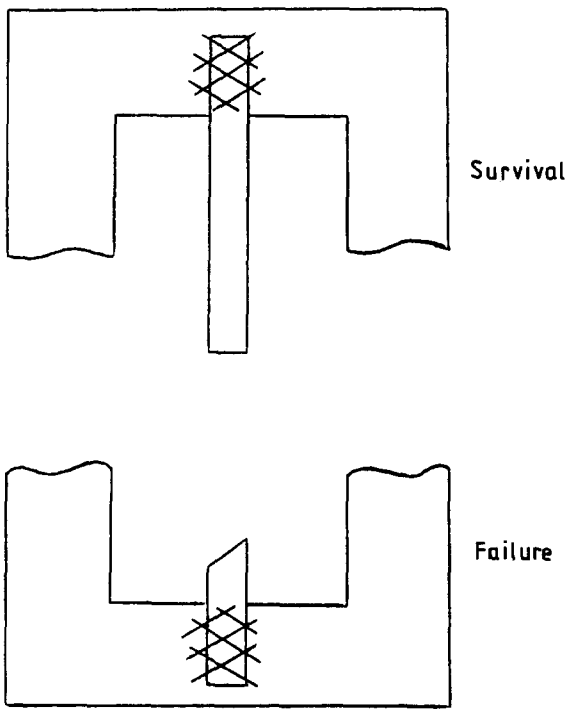

Figure 4 Interpretation of the recoil test.

TABLE I Recoil compression test results for Thornel P130 carbon fibre.

Applied load (cN)	Top failure	Bottom failure	Applied stress (MPa)
2.58	0	0	319
2.66	0	0	328
2.67	0	0	329
2.68	1	0	330
2.80	0	0	346
2.94	0	0	363
3.02	1	1	372
3.04	1	1	376
3.05	1	0	376
3.07	0	0	379
3.08	0	0	381
3.09	1	1	382
3.28	1	1	405
3.35	1	1	413
3.42	0	0	422
3.49	1	1	431
3.51	0	0	433
3.54	1	1	437
3.55	0	1	439
3.60	1	1	444
3.61	1	1	445
3.63	0	0	448
3.67	1	1	453
3.74	1	1	461
3.85	1	1	475
3.99	1	1	492

Note: 0 corresponds to survival and 1 corresponds to failure.

to reduce bias. Because these methods used to estimate the recoil compressive strengths of carbon fibres are not based on rigorous statistical principles, either method can be used for comparative analysis. Therefore, except where noted in graphical comparisons, all compressive strength data reported in this work were determined by the second method, the method of Wang *et al.* [8].

Although the data analysis techniques described above are not based on rigorous statistical principles, statistical methods are available to handle recoil data, which are a type of stimulus-response data (also known as all-or-nothing, quantal or, more commonly, binary response data) [11]. During the recoil test, each half of the fibre exhibits a binary response (a survival or failure) to a certain dose or stimulus level (the applied load). Therefore, the data can be grouped into stress levels or ranges and analysed with Weibull statistics. However, when merely the median recoil compressive strength is of interest, it has been shown that the value obtained using the two methods described in the present work agrees closely with that calculated from a statistically based analysis [11].

3. Results and discussion

3.1. Tensile testing results

Fig. 5a, a plot of manufacturer-supplied data on the tensile strength as a function of Young's modulus for Thornel and Fiber G pitch-based carbon fibre, suggests that textural and microstructural differences affect the tensile properties of these carbon fibres. It should be noted that the data presented in Fig. 5a are not directly comparable because the two manufacturers report tensile data differently: Amoco reports strand data, whereas du Pont reports single-filament data. Therefore, at the beginning of the current study, single-filament tensile tests were performed on these fibres. The results of the single-filament tensile testing, presented in Fig. 5b with 95% confidence intervals for the tensile strength, indicated that the single-filament tensile properties of carbon fibres can differ from the values supplied by the fibre manufacturers. Fig. 5b also indicated that the tensile strengths of fibres with a folded-radial texture were greater than the tensile strengths of the fibres with a flat-layer texture.

3.2. Comparison of recoil initiation techniques

As described earlier, the recoil test is initiated by cutting or ionizing the stressed carbon fibre at the midpoint of the gauge length. The method employed to induce this initiation can affect the results of the recoil test. For example, if the initiation technique imparts a lateral stress or displacement, the fibre may be exposed to lateral shear stresses or bending stresses as well as the assumed compressive stress.

In the first part of this study, the mechanical and electrical initiation techniques were compared for two different fibre types, Thornel P55 and P75. Because the P55 data cover a wide stress range, the results of these tests are presented in Fig. 6 by the graphical

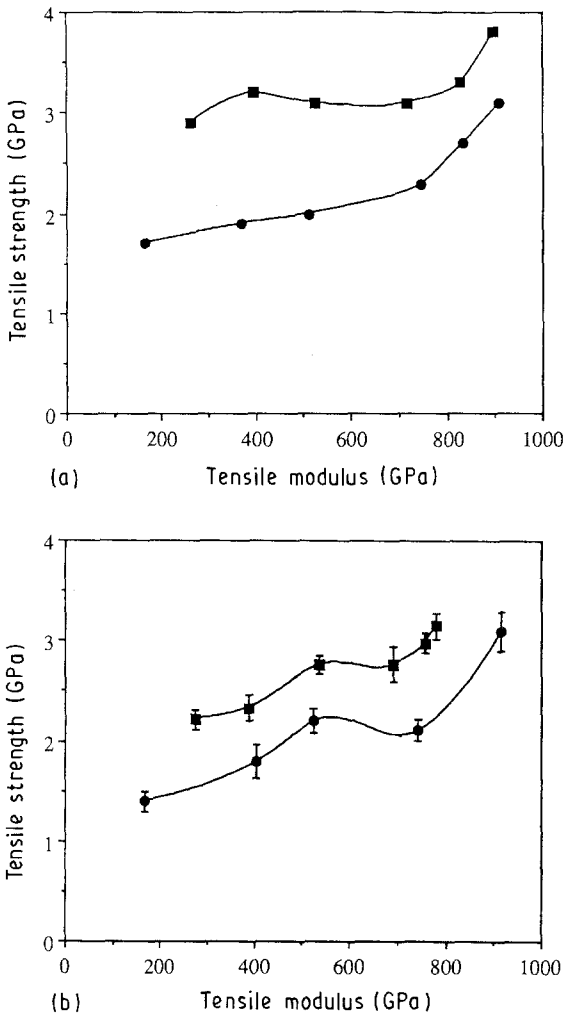

Figure 5 The mechanical properties of (●) Thornel and (■) Fiber G pitch-based carbon fibres: (a) manufacturer's supplied data, and (b) single-filament tensile test data.

method of Park [9]. Although not presented here, the results for the P75 fibre show the same trends as the P55 data. As Fig. 6 shows, both initiation techniques produced compressive failures beginning at approximately 350 MPa. For the mechanical initiation technique, recoil compressive failures occurred for all fibres tested when the applied stress level exceeded 650 MPa. However, when the electrical initiation technique was used, a stress level over 1000 MPa was required to produce recoil compressive failures in 100% of the fibres. These results suggest that one or both methods introduce a bias in the data. The recoil compressive strength of the P55 fibre was 490 MPa using the mechanical initiation technique, and was 810 MPa using the electrical initiation technique. These values were determined by following Park's data analysis procedure [9], as previously discussed. The electrical method was selected to initiate the recoil in all subsequent tests in this research because it was easier to perform and it was not sensitive to the influence of the operator's skill level.

3.3. Recoil strength comparison

In this part of the present investigation, the recoil compressive strengths of Thornel and Fiber G pitch-

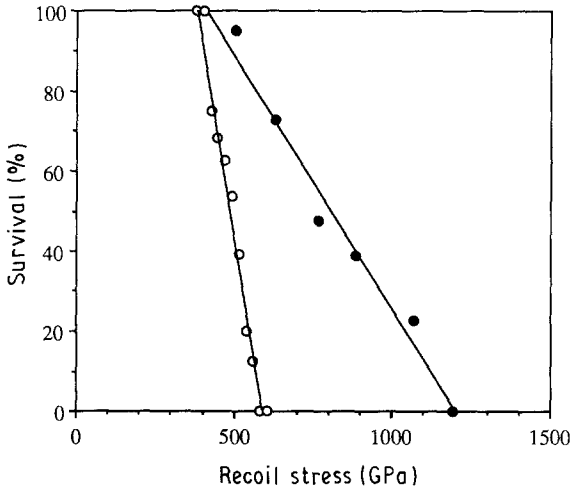

Figure 6 Comparison of recoil test initiation techniques. (●) Electrical initiation, (○) mechanical initiation.

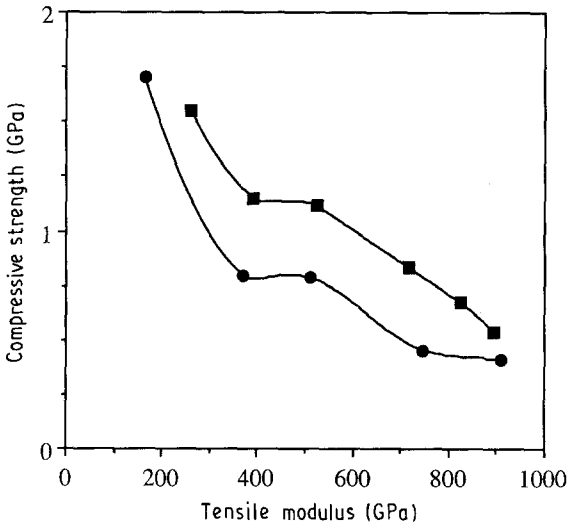

Figure 7 Recoil compressive strength of (●) Thornel and (■) Fiber G as a function of Young's modulus.

based carbon fibres were compared. Table II presents the results of these recoil tests, together with the manufacturers' supplied tensile data and the tensile data obtained from single-filament tensile testing conducted at Clemson. Note that the fibre manufacturers supplied tensile data obtained by different test procedures; Du Pont supplied average single-filament tensile data, whereas Amoco supplied strand tests data. As indicated in Table II, the recoil compressive strength of Fiber G carbon fibres was superior to the recoil compressive strength of Thornel carbon fibres at each modulus level tested. The tensile and recoil properties of Amoco P120 fibres were not obtained because these fibres could not be separated in sufficient quantities and lengths for single-filament testing.

During the testing of Thornel P25 fibres, it was necessary to apply stresses on individual fibres that equalled or exceeded the average tensile strength of P25. In fact, approximately one-third of the tested P25 fibres failed because their individual tensile strengths were exceeded. When these fibres were examined, it was noted that both ends exhibited compressive failures as defined earlier. The remaining two-thirds of the P25 fibres were tested by the recoil method, but there was no trend in the number of compressive failures observed as the applied load increased. Therefore, the recoil compressive strength calculated for P25 is indicated as being equal to or greater than its tensile strength.

A graphical presentation of the recoil compressive strength as a function of Young's modulus is presented in Fig. 7 (in this figure, the modulus values were obtained from the single-filament tests conducted at Clemson). This figure clearly shows that the recoil compressive strength decreased as the modulus increased. Fig. 7 also shows that the recoil compressive strength of Fiber G pitch-based carbon fibre was superior to the recoil compressive strength of Thornel pitch-based carbon fibre at each modulus level. Similar trends have been reported for composite compression strengths for these fibre types [1]. At first glance, the recoil compressive strengths of the high-modulus fibres appear to be closer together than those

TABLE II Pitch-based carbon fibre mechanical properties

Fibre	Tensile strength[a] (GPa)	Tensile modulus[a] (GPa)	Tensile strength[b] (GPa)	Tensile modulus[b] (GPa)	Compressive strength[c] (GPa)
Fibre G					
E35	2.9	262	2.2	275	1.6
E55	3.2	393	2.3	387	1.1
E75	3.1	524	2.8	537	1.1
E105	3.1	717	2.8	692	0.8
E120	3.3	827	3.0	756	0.7
E130	3.8	896	3.1	780	0.5
Thornel					
P25	1.7	165	1.4	166	1.4[d]
P55	1.9	368	1.8	403	0.8
P75	2.0	510	2.2	525	0.8
P100	2.3	745	2.1	742	0.5
P120	2.7	834	-	-	-
P130[e]	3.1	910	3.1	915	0.4

[a] E.I. du Pont de Nemours & Co., single-filament tensile data and Amoco Performance Products, Inc., strand tensile data.
[b] Single-filament tensile data (40 mm guage length, corrected for machine compliance).
[c] Recoil compressive strength from present investigation.
[d] Compressive strength equal to or greater than tensile strength.
[e] Amoco Performance Products, Inc. experimental fibre.

of the low-modulus fibres. However, as Fig. 8 shows, the range over which the failures were observed was much smaller at the high modulus levels than at the low modulus levels. Therefore, the difference in strengths between Thornel and Fiber G high-modulus fibres was significant. An interesting observation from Fig. 7 is that a slight flattening of the data occurred for both manufacturers' fibres in the 350–500 GPa modulus range. This unexplained phenomenon has been observed in the data of other investigators [3] for Thornel pitch-based fibres.

3.4. SEM examination of recoil failure surfaces

The typical compressive failure mode for pitch-based carbon fibres is shear. Fig. 9 is a photograph of the shear mode compressive failure of an Amoco P55

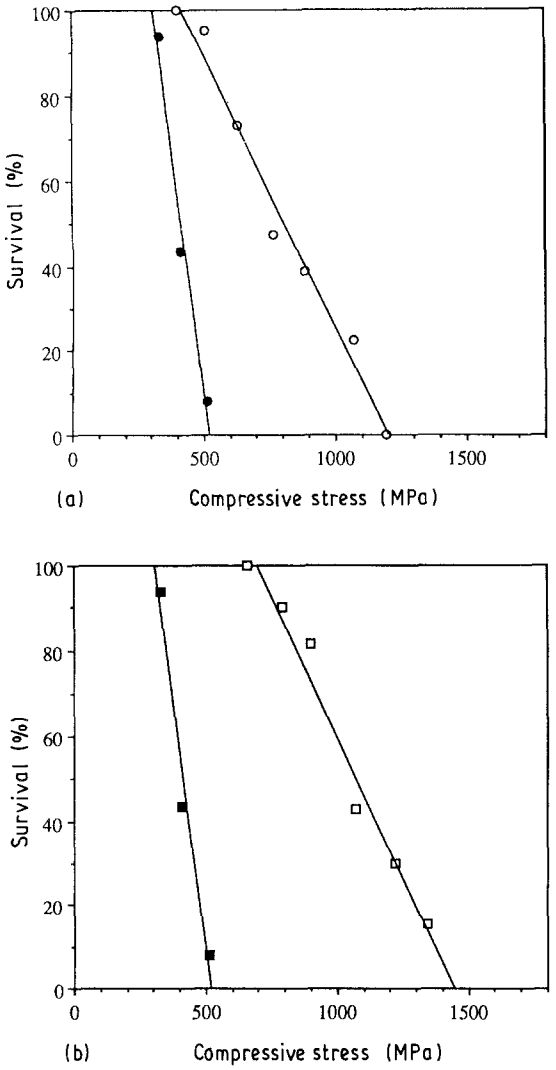

Figure 8 Comparison of the stress ranges of compressive failure for (a) Thornel and (b) Fiber G pitch-based carbon fibres. (●) P130, (○) P55, (■) E130, (□) E55.

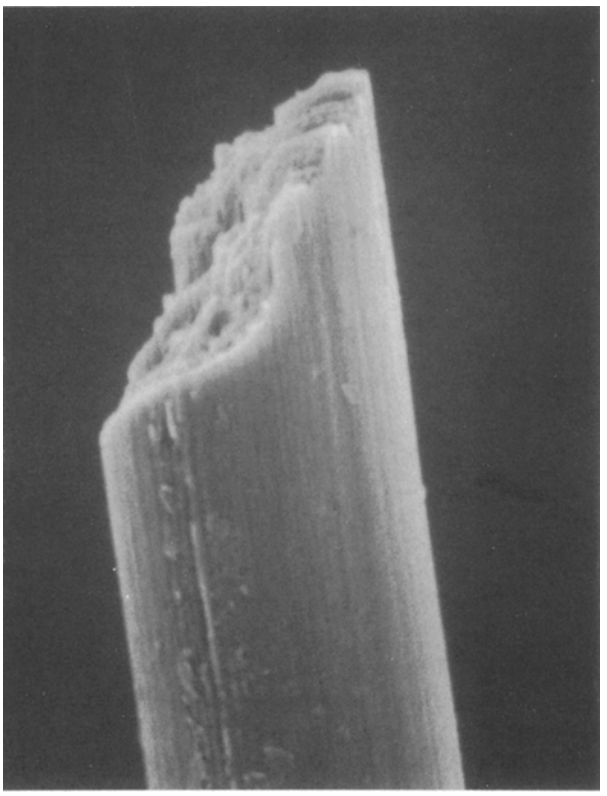

Figure 9 Compressive failure of Thornel P55 carbon fibre.

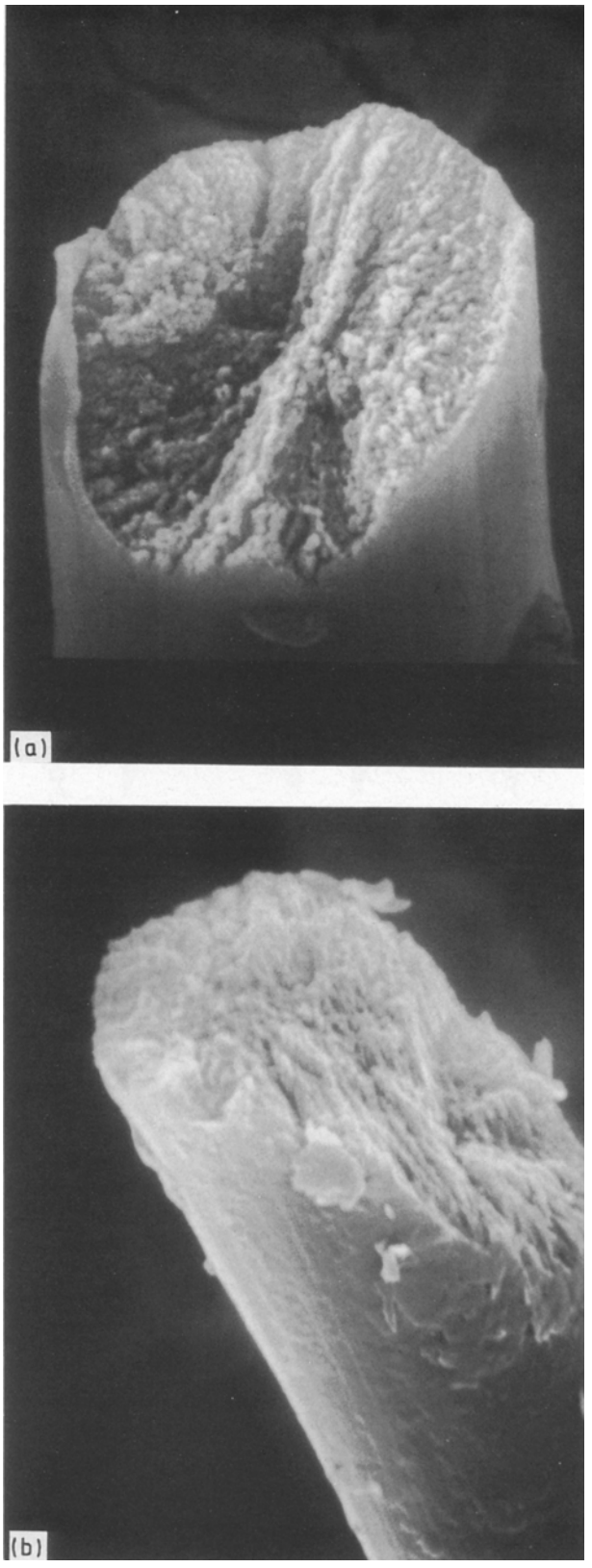

Figure 10 Compression failure surfaces observed in Thornel P25 carbon fibre.

fibre. This photograph shows the 45° shear failure which was observed in most of the Amoco fibres with a 403 GPa (55×10^6p.s.i.) modulus and higher. The failure mode of the low modulus P25 fibre was observed to be either a flat failure surface or a combina-

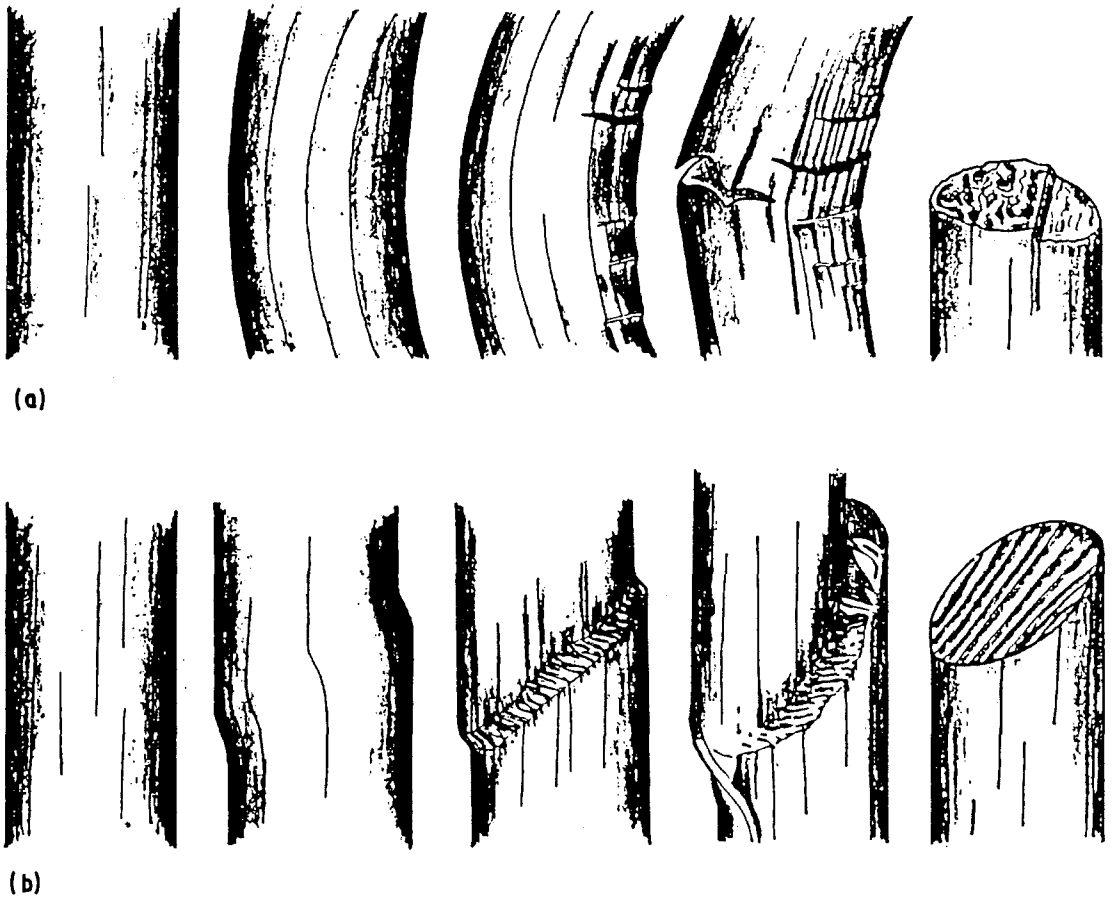

Figure 11 Proposed failure mechanism for (a) PAN-based and low-modulus pitch-based carbon fibres and (b) high-modulus pitch-based carbon fibres. Dobb *et al.* [2].

tion of this flat failure surface and a compressive shear failure. These failure surfaces are shown in Fig. 10. These observations agree well with the findings of other researchers who have described the failure mechanisms of carbon fibres experiencing recoil compression loading conditions [3].

Dobb *et al.* [3] proposed a failure scenario based on the differences in the failure modes observed for low- and high-modulus carbon fibres. Fig. 11 shows the failure mechanisms proposed by these researchers. These mechanisms were postulated after examining both pitch-based and PAN-based carbon fibres that were exposed to recoil stresses. The failure sequence observed for low-modulus fibres due to recoil loading is shown in Fig. 11a. As the recoil compressive load increases, the fibre begins to buckle with the formation of kink bands. With additional load, a tensile crack forms on the tension side of the buckled fibre, and the kink bands propagate inwards. Finally, the tensile crack and the kink bands meet and failure occurs. The failure mechanism for the high-modulus fibres is shown in Fig. 11b. In this case, the initial recoil compressive load causes kink bands to develop across the entire fibre by simple shear deformation. Then the fracture simply propagates along the kink band. Dobb *et al.* [3] suggested that the low recoil compressive strength of the high-modulus fibres was caused by their high degree of orientation and sheet-like flat-layer texture, which might be less resistant to shear across basal planes than the more random structure that is typical of the low modulus fibre.

Microscopic examination of the failure surfaces of Fiber G pitch-based carbon fibres revealed that most of the fibres, in all modulus ranges, failed with flat failure surfaces, (typical of the failures observed in Amoco's low-modulus Thornel fibres). This observation only applies to the portion of the fibre in the gauge length. It is possible that the folded-radial texture of the Fiber G carbon fibre may have influenced its failure mechanism by inhibiting the shear failure which is typical of brittle pitch-based carbon fibres. However, when the support matrix (glue) was removed from the fibre after compression testing, microscopic analysis of the region beneath the matrix revealed many poorly defined shear faces in the Fiber G carbon fibre, as indicated in Fig. 12a. For the Fiber G carbon fibres, there did not seem to be a clear-cut cleavage plane, as observed in the Thornel fibres of Fig. 12 c,d. Instead, the photographs indicated that the failure of Fiber G carbon fibre initiated as a shear deformation followed by total shear failure. Fig. 12b is a photograph of a high-modulus (E120) Fiber G carbon fibre with the support matrix removed. This picture indicated that even the high-modulus du Pont fibres experienced some buckling prior to failure, another indication that these fibres resist the shear failure mechanism.

The analysis of the failed fibres after removing the support matrix provided some interesting information on the behaviour of supported fibres under compressive loading. Unfortunately, these findings also indicate that the assumption of totally reflected

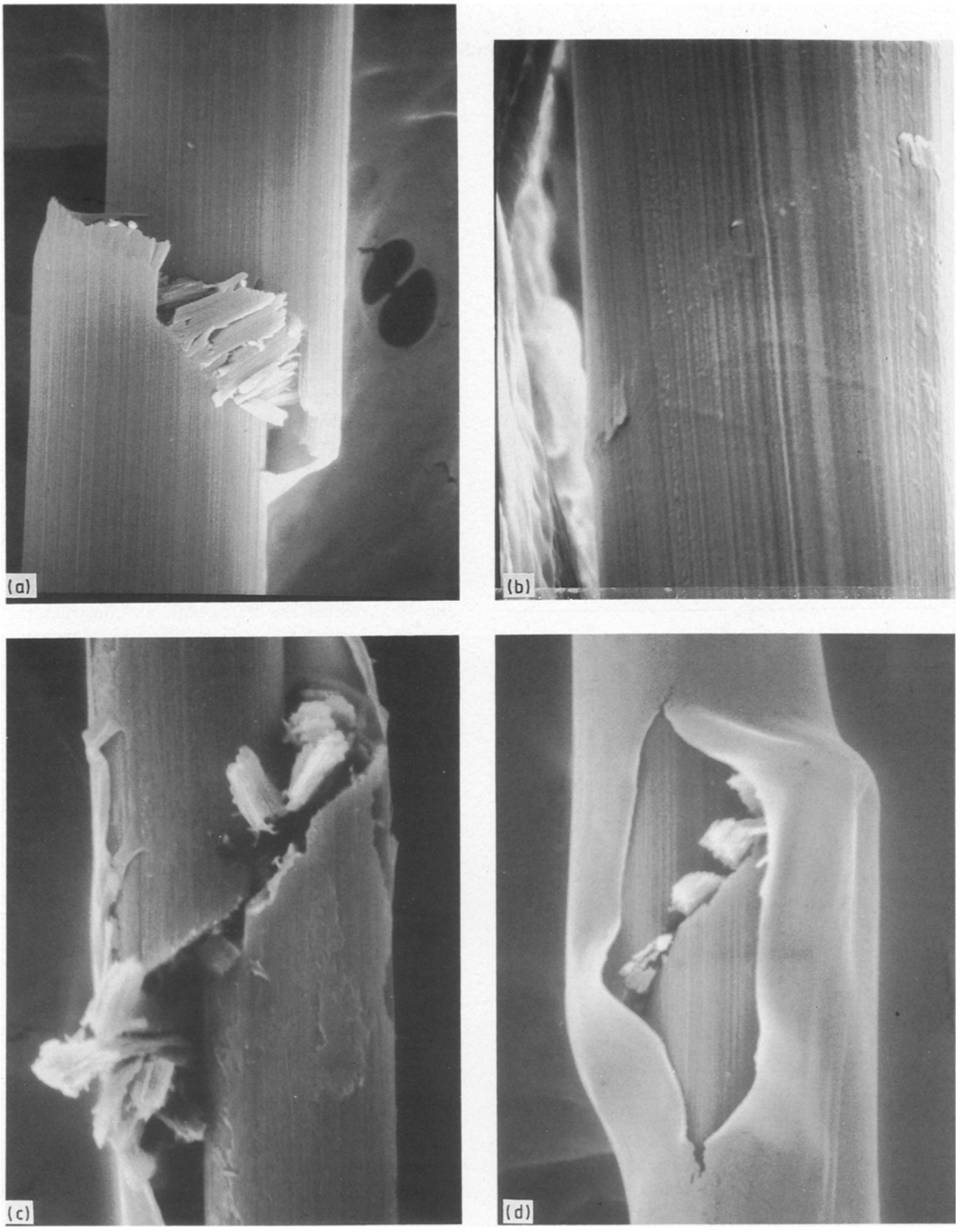

Figure 12 Compression failure surfaces observed beneath the support matrix: (a) poorly defined shear failure observed in Fiber G carbon fibre; (b) shear deformation and buckling observed in Fiber G carbon fibre; (c, d) well-defined shear failure observed in Thornel carbon fibre. Support matrix has been dissolved to reveal carbon fibre.

stresses at the grip may not be true. Thus, reported values of recoil compressive strengths may be overstated because some of the strain energy is absorbed as the fibre fails in the support matrix.

3.5. Proposed failure model for recoil test

Observations of the failure surfaces of carbon fibres which have experienced critical recoil compressive loads indicated that the fibres may have bent slightly before either buckling or shearing occurred. Also, some of the fracture surfaces observed in this work indicated that low-modulus fibres failed with a combined tensile and compressive failure surface. This conclusion is supported by the work of Kumar [12] in which carbon fibres were fractured by bending and then carefully collected and examined. During SEM

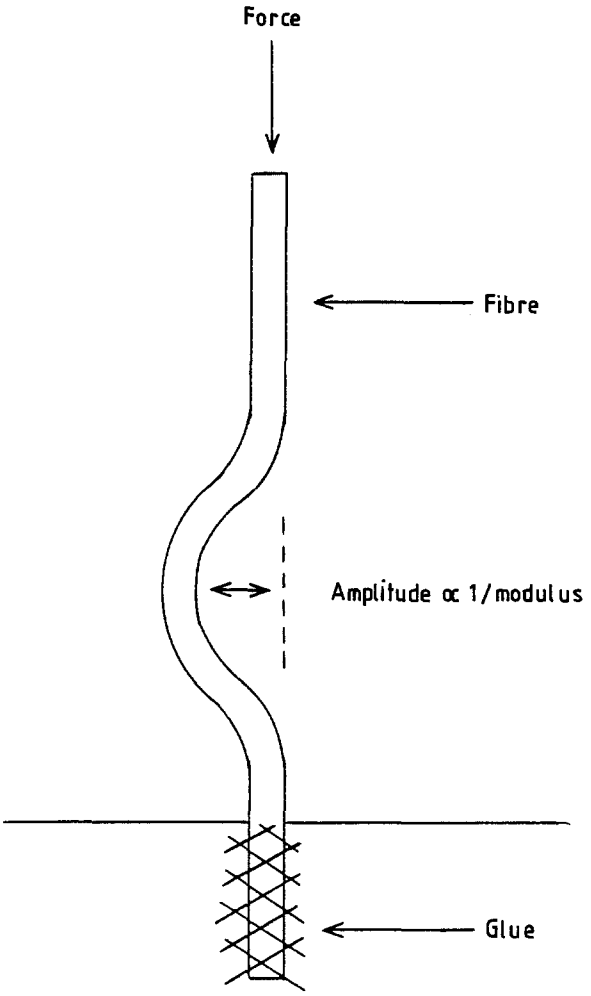

Figure 13 Proposed displacement model for a carbon fibre during the recoil test. Figure presents the inverse relationship between displacement wave amplitude and fibre Young's modulus.

examination, the portions of the fibres that were in tension and the portions that were in compression were shown to have different failure surfaces. Therefore, the findings of Kumar [12] support the present claims that a combined failure occurs in the lower modulus fibres.

In the original assumptions and analysis of the stress profile of a fibre in the recoil test, Allen [4] assumed that there was no lateral displacement of the fibre, and therefore, conducted a one-dimensional analysis. However, this research indicates that during the conversion of the strain energy to kinetic energy, a macroscopic lateral displacement may result due to the dimensions of the test specimen (Euler bending). Therefore, as this lateral displacement travels along the fibre length with the zero stress front, it will exhibit some characteristic wavelength and amplitude. Dobb *et al.* [3] also reported that during the recoil test, the moving stress trajectory in the fibre is not purely uniaxial. As this hypothetical wave approaches the constrained (mounted and gripped) fibre end, it imparts a shear stress. The shear stress increases as the wave approaches the constrained end until a shear failure or a combined tensile and shear failure occurs.

This scenario could explain the combined failure mode observed in the low-modulus fibres. However, it does not explain the lack of combined failure modes in the high-modulus fibres. If the amplitude of the wave is smaller for the higher modulus fibres, fewer mixed-mode failures might be observed. If only one failure mode is involved, a sharper transition from survival to failure in the recoil test would be expected. Indeed this is the case. As seen in Fig. 8, the transition from survival to failure for the high-modulus fibres covered a much smaller stress range than the low-modulus fibres for both Thornel and Fiber G pitch-based carbon fibres. These observations suggest an inverse relationship between the fibre stiffness, E, and wave amplitude, as indicated in Fig. 13. If this phenomenon is related to the fibre's resistance to bending, then the inverse relationship will include the fibre's moment of inertia, I, in the form of the bending stiffness, EI. Inclusion of the moment of inertia term in this relationship may also explain how varying the shape of the fibre could improve its resistance to buckling failure in compression [13].

Crasto and Kumar [10] also reported that carbon fibres may fail due to flexure in the recoil test method. However, they hypothesized that the flexural stress components arise as a result of the finite time required to cut through the fibre from one side to the other. Also, in an effort to damp this flexural stress component, they treated the fibres with a "nonstructural" coating consisting of a solvent with a low concentration of silicone grease. As a result of this treatment, the calculated recoil compressive strength of Amoco's Thornel pitch-based carbon fibres increased by 60%–100% percent over the recoil compressive strengths of the uncoated fibres. The recoil compressive strengths of these coated fibres also exceeded the composite compressive strengths of the fibres. By varying the gauge length, Crasto and Kumar [10] demonstrated that the coating does not increase the recoil compressive strength by absorbing energy. These results can be applied to the present interpretation of the recoil test shown in Fig. 13. Basically, the coating adds to the stiffness term and, therefore, decreases the amplitude of the displacement wave.

4. Conclusions

In the present investigation, the compressive strengths of pitch-based carbon fibres manufactured by Amoco Performance Products, Inc. and E. I. du Pont de Nemours & Co. Inc. were compared. Using the recoil test method, it was shown that the recoil compressive strengths of du Pont's Fiber G pitch-based carbon fibres were superior to Amoco's Thornel pitch-based carbon fibres at all modulus levels. Analysis of the failed fibre ends revealed that the texture of du Pont's fibres may have inhibited shearing of the basal planes and thus increased their compressive strengths. The compressive strength of Thornel P25 could not be determined by the recoil method because the applied compressive stress level was limited by the tensile strength.

An evaluation of the recoil test method revealed that, as the underlying assumptions of this test method require, the strain energy is not reflected totally at the gripped end of the fibre. However, it was demon-

strated that the recoil test can be used to compare the compressive strength of different fibres, provided the same data analysis technique and recoil initiation method is used. Analysis of recoil test initiation methods demonstrated that the calculated compressive strength is dependent on the initiation method. The electrical initiation method was selected for this investigation because it was easier to implement and because it was insensitive to the skill level of the person conducting the test.

Microscopic analysis of the fibre cross-sections revealed that some low-modulus pitch-based carbon fibres exhibit a dual failure mode. High-modulus fibres, on the other hand, exhibit a shear failure mode typical of brittle materials. These observations were incorporated into a model for the displacement of a single filament in the recoil test. Basically, a lateral displacement wave was proposed which travels with the stress wave down the fibre length. It was reasoned that the amplitude of this wave is inversely dependent on the modulus and moment of inertia of the fibre. Analysis of the variation or spread of the recoil test data provided additional evidence to support the proposed model.

Acknowledgements

The authors thank Professor D. J. Johnson, Chair of Textiles M. G. Dobb and Dr C. R. Park of Leeds University, and Professor S. Kumar, Georgia Institute of Technology, for advice in developing the recoil test method; Angelia Smith for assistance in performing the recoil tests; Amoco Performance Products, Inc. and E. I. du Pont de Nemours & Co. Inc. for supplying the pitch-based carbon fibre used in this study; and Chapman and Hall Ltd, for permission to reproduce Figs 1 and 11.

References

1. A. S. CRASTO and D. P. ANDERSON in Proceedings of the American Society for Composites, 5th Technical Conference on Composite Materials", East Lansing, MI, June 1990 (Technomic, Lancaster, PA, 1990) p. 809.
2. M. ENDO, *J. Mater. Sci.* **23** (1988) 598.
3. M. G. DOBB, D. J. JOHNSON and C. R. PARK, *ibid.* **25** (1990) 829.
4. S. R. ALLEN, *ibid.* **22** (1988) 853.
5. M. ENDO, personal communication (1990).
6. ASTM D3379-75, "Standard Test Method for Tensile Strength and Young's Modulus for High-Modulus Single-Filament Materials", Vol. 15.03 (American Society for Testing and Materials, Philadelphia, PA, 1989) p. 127.
7. C. LI and N. R. LANGLEY, *J. Amer. Ceram. Soc.* **68** (8) (1985) C-202.
8. C. S. WANG, S. J. BAI and B. P. RICE, in "Proceedings of the American Chemical Society", Vol. 61, Division of Polymeric Materials: Science and Engineering, Miami, FL, 1989 (ACS, 1989) p. 550.
9. C. R. PARK, PhD thesis, University of Leeds (1990).
10. A. S. CRASTO and S. KUMAR, *SAMPE Proc.* **35** (1990) 318. 318.
11. G. J. HAYES, D. D. EDIE and S. D. DURHAM, in "Twentieth Biennial Conference on Carbon, Extended Abstracts", Santa Barbara, CA, June 1991 (American Carbon Society, 1991) p. 326.
12. S. KUMAR, personal communication (1989).
13. E. G. STONER, D. D. EDIE and J. M. KENNEDY, *High Temp. High Press.* **22** (1990) 229.

Received 25 March
and accepted 20 November 1992